nature climate change

SUPPLEMENTARY INFORMATION

DOI: 10.1038/NCLIMATE3394

In the format provided by the authors and unedited.

Potential volcanic impacts on future climate variability

Ingo Bethke[1]*, Stephen Outten[2], Odd Helge Otterå[1], Ed Hawkins[3], Sebastian Wagner[4], Michael Sigl[5,6] and Peter Thorne[7]

[1]Uni Research Climate, Bjerknes Centre for Climate Research, Bergen 5007, Norway. [2]Nansen Environmental and Remote Sensing Center, Bjerknes Centre for Climate Research, Bergen 5006, Norway. [3]NCAS-Climate, Department of Meteorology, University of Reading, Reading RG6 6BB, UK. [4]Institute for Coastal Research, Helmholtz-Zentrum Geesthacht, Geesthacht 21502, Germany. [5]Laboratory of Environmental Chemistry, Paul Scherrer Institute, Villigen 5232, Switzerland. [6]Oeschger Centre for Climate Change Research, University of Bern, Bern 3012, Switzerland. [7]Irish Climate Analysis and Research Units, Department of Geography, National University of Ireland Maynooth, Maynooth, County Kildare, Ireland. *e-mail: ingo.bethke@uni.no

The Supplementary Information primarily provides further detail and discussion that was not possible to cover in the main text. It also contains several tables and figures referred to in the main text and online methods.

Historical volcanic activity.
There exist various sources of estimates of volcanic forcing[1-4]. We utilise a set of estimates arising from ice-cores as detailed in the online methods which further describe how the 2,500 year series[4] is resampled to create plausible 21st century climate forcing futures. The original proxy-based series are shown in Supplementary Figure 1. This figure highlights that there exists considerable variability in volcanic forcing through time. The centennial-mean burden historically has varied by a factor of five, and the twentieth century was towards the low-end of the range of 25 centennial samples available. The thirteenth century had the most extreme behaviour with no fewer than 4 eruptions that exceeded the magnitude of the recent Mt. Pinatubo eruption in 1991 (which itself was the largest 20th century event). The three most extreme members from the 60-member ensemble exceed slightly the thirteenth century time-averaged burden (cf. Figure 1 in the main text), but such exceedance would be expected by chance. This serves to reinforce how relatively quiescent the 20th century was and how poor a guide it may be to future volcanic effects.

Realism of future volcanic forcing.
Our construction of plausible volcanic forcing oversimplifies real world volcanism, and there is potential to refine the statistical representation of past volcanic activity in terms of frequencies, magnitudes and geographic locations. The resampling approach does not account for small eruptions that are not captured in ice-cores and provides a poor statistical representation of the very large eruptions that have only a few occurrences in the 2,500-year-long record[4] (Supplementary Fig. 1). Indeed, a comparison of our plausible forcing with the original reconstruction indicates that the largest eruptions are potentially over-represented in our forcing.

The statistics of reconstructed past and synthetic future volcanic activity are compared in Supplementary Figure 2, which shows eruption frequencies for five selected size classes (panel a) and three geographical regions (panel b) of reconstructed past and synthetic future volcanic activity. While all frequencies of the future forcings fall within the 5-95% sampling uncertainty range of the frequencies found in the reconstruction, the statistics indicate that our future forcing ensemble by chance may over-represent the largest, Samalas-like eruptions and under-represent Mt. Pinatubo-like eruptions as well as extratropical Northern Hemisphere eruptions. After excluding the five strongest forcing members, the frequency of very large eruptions in the synthetic forcing better matches that of the reconstruction. However, by construction the ensemble is consistent with the underlying observed distribution which implies that we cannot exclude the possibility that a scenario akin to one of these five extreme members constructed may actually occur. The inclusion or exclusion of the strongest forcing members has a measurable impact on the results but does not qualitatively change the principal outcomes of the study (Supplementary Table 1).

Since the relationship of ice-core sulphate concentrations and stratospheric aerosol loading is unknown for eruptions larger than Pinatubo (1991) the latter is more uncertain for very large eruptions (e.g., Tambora 1815, Samalas 1257). Microphysics suggests that larger SO_2 injections produce larger aerosol sizes with smaller radiative effects per mass unit sulphur[5]. Thus, the linear Gao et al.[1] scaling may overestimate the radiative effects of the largest eruptions in our model because the radiative effects are smaller for increased aerosol sizes[5]. Crowley et al.[2] suggested a 2/3 power scaling for eruptions larger than Mt. Pinatubo to mitigate these effects, something that should be considered in future applications. While further research is required to better constrain the forcing of very large eruptions, our ice-core based volcanic forcing is to first-order proportional to relevant surface temperature reconstructions[4,6]. In this study, the potentially too low sensitivity of the model and too strong forcing from large eruptions partly compensate each other. Nevertheless, we likely underestimate the effects of small-to-medium size eruptions and may overestimate the effects of the largest eruptions.

These and other aspects may be improved in future through use of more sophisticated forcing models based on extreme value theory[7,8], combined with longer records and improved understanding of large volcanic eruptions[9].

Impact of ensemble size on statistical robustness.
Given limited ensemble sizes, a concern is whether the quantified, volcanic induced changes in probability density functions are robust over time. We tentatively addressed this point by comparing the ensemble standard-deviation of annual-mean volcanic aerosol load with the ensemble standard-deviation of annual-mean surface temperature (Supplementary Fig. 3). The temporal variability in the ensemble spread of the volcanic aerosol load (panel a) illustrates that considering individual years, 60 forcing futures are not sufficient for obtaining stationary ensemble statistics. The corresponding temporal variability for surface temperature (panel b) tends to follow that of volcanic aerosol load, illustrating how under-sampling of volcanic forcing possibilities affects the projection outcome. Given the episodic and short-lived nature of the forcing, we cannot expect that 60 forcing members are sufficient for providing a good probabilistic representation on annual resolution possibilities (i.e. for each individual year). It is thus unsurprising that the GMST spread of VOLC is uneven in time (Fig. 2a) and roughly mirrors the evolution of the ensemble mean of volcanic aerosol load (Supplementary Fig. 3a). Climate impact assessments are advised to use sufficiently large time-windows in their computation of ensemble statistics to mitigate the problem.

A challenge remains that the ensemble must be large enough to adequately sample both volcanic forcing possibilities and internal climate variability. Having only one simulation per forcing possibility thus may compromise capturing combined effects[10,11].

Changes in distribution statistics.
Supplementary Table 1 provides standard distributional statistics and summarizes quantitatively the impacts presented in the main article. For all climate variables assessed in the table, the distributional means of NO-VOLC significantly differ from those of VOLC-CONST and VOLC, which, in turn, are very similar to each other. This result gives confidence in the application of a constant background volcanic forcing in future climate simulations if the main goal is to correctly predict the centennial mean shifts of the distributions. Conversely, the variance of VOLC significantly differs from those of NO-VOLC and VOLC-CONST, which, in turn, are very similar to each other. Thus, the

consideration of realistic volcanic forcing behaviour affects also the shape of distributions and has a demonstrable impact on temporal climate variability and therefore uncertainty ranges of climate projections.

Assessing model sensitivity.
Our results are based on a single model system, which has its own particular deficiencies in the representation of the forced climate response and internal climate.

The comparison of the simulated to observed global temperature change following the Mt. Pinatubo eruption (see Methods for experimental details) reveals a low bias of the global climate sensitivity of the model (Supplementary Fig. 4). The ensemble-mean net radiative effect at the top of the atmosphere of 2.2 W/m^2 (panel c) is 20% lower than observed but still within the uncertainty range of observational estimates[12] of 2.7±1 W/m^2 and towards the lower range of the 2–4 W/m^2 spread of CMIP5 models[13]. The ensemble-mean maximum global surface cooling after Mt. Pinatubo eruption of 0.3 K (panel b) is 25% lower than ENSO-corrected observational estimates of 0.4 K[14,15] and more than 50% lower than the ENSO-corrected lower troposphere estimate of 0.7 K[16].

The simulated land precipitation response one year after Mt. Pinatubo eruption indicates a large-scale weakening of the East Asian summer monsoon that is consistent with previous findings[17,18] (Supplementary Fig. 5). The summer precipitation response over the Sahelian region is, in contrast, less strong than results of previous studies would suggest[19]. The latter is indicative for a low sensitivity of the simulated variability in the position of Intertropical Convergence Zone, which strongly influences Sahelian rainfall variability, to volcanic forcing in our model. Like other climate models, our model generally underestimates the volcanic impact on precipitation[20].

Previous studies[13,21] found that current climate models – including NorESM – have problems to reproduce the observed atmospheric circulation response to tropical eruptions that leads to a winter time warming over the Northern Hemisphere continents. More recent studies[22,23] partially recovered the observed response after limiting the analysis of the model output to the first winter and to the largest eruptions of the late 19th century and 20st century. In addition, the low-top of the atmospheric model may affect the dynamical response, but there is no evidence that high-top models produce a more realistic response[24]. Deficiencies in the atmospheric circulation response might have a small global effect, but may become important for regional projections and partly explain a weak ocean circulation response in our simulations.

Ocean circulation biases that cause overly efficient ocean heat uptake[25] lead to a strong anthropogenic signal in steric sea level rise that potentially masks the volcanic impact. Despite the existence of such biases, the impacts of volcanic activity on the ocean circulation variability in our model agree well with those simulated by others models[26].

The volcanic impacts on climate variability may also depend on existence and strength of an ENSO response. Our model does not simulate a robust ENSO response to Mt. Pinatubo forcing[12], supporting the absence of a causal relation between the 1991 Mt. Pinatubo eruption and the subsequent El Niño event[27]. In turn, strong extratropical eruptions have been found to cause a robust ENSO response in our model[28].

The evidence for a low bias in NorESM's sensitivity to volcanic forcing by no means reduces the relevance of the simulation findings. On the contrary, it indicates that the role of volcanic effects may be larger than suggested in this study. A potential overrepresentation of largest eruptions by chance due to sampling and also due to the linear scaling that we applied to obtain the forcing (prior Sections) may, however, partially compensate for the low model sensitivity.

Robustness of findings to errors in volcanic sensitivity and anthropogenic trend. Another source of uncertainty stems from the simulated anthropogenic trend that depends on the choice of the anthropogenic greenhouse gas scenario and the model's sensitivity to the anthropogenic forcing. We would note that the anthropogenic concentration scenario RCP4.5[29] is more pessimistic than the 2 K goal of the Paris agreement[30], consistent with which our simulated warming by end of Century exceeds 2.5 K (Fig. 2a), despite the low model sensitivity[25]. In light of the Paris agreement, we deemed RCP4.5 the most likely scenario of the available RCP scenarios. RCP dependence combined with deficiencies in the model response are nevertheless expected to have some effect on the results.

The dependence on the anthropogenic trend is most obvious if measuring volcanic effects relative to the anthropogenic climate change – like this study does for GMST and global sea level rise – in which case the volcanic signal is expected to become relatively weaker for a stronger anthropogenic trend. However, the presence of the anthropogenic trend does not diminish the signal strength of volcanic effects in the same way as internal variability does since the anthropogenic trend can be estimated (within uncertainty bounds) and removed from the analysis. Thus, this effect is likely relatively small and we believe the most important aspects of the study to be relatively insensitive to plausible anthropogenic emissions futures such that our principal conclusions would still hold if one picked a different RCP scenario. The same may also be expected to hold for another model with a different climate sensitivity, although we would encourage one or more modelling groups to undertake such experimentation to confirm this. We would stress that despite potentially lower relative signal strength, volcanic induced climate variability would, all else being equal, become more important in a high RCP world that is more vulnerable due to higher existent stresses on society.

It is reasonable to assume that the volcanic effects on annual-to-decadal scale variability – manifesting in an increase of ensemble spread – are to first order insensitive to the anthropogenic background trend. Our results suggest volcanic effects increase the range of annual to decadal variations, while anthropogenic change primarily shifts the entire distribution. It is this increase in range – between negative and positive temperature extremes – that the study highlights. However, the global warming dependence of the volcanic impact on local extremes might be more non-linear and complex than implied herein. This should be addressed in future studies that focus more on regional climate impacts.

For certain diagnostics we considered – like the probability of decade-long negative GMST trends – volcanic effects become relatively more important under a stronger anthropogenic scenario, because internal, unforced climate variability is less likely to offset the anthropogenic trend. The same holds for ‘pauses’ in sea level rise and Arctic sea ice decline. Nonetheless, for other quantities one would expect a relatively weaker volcanic signal if one used a stronger anthropogenic emission scenario. For example, the volcanic effects on the time when GMST change exceeds 1.5 K can be expected to be sensitive to the background

trend. However, there is only little difference between the RCP scenarios early in the century (Knutti & Sedlacek[31], their Fig. 1). Similarly, the volcanic effects on the time of emergence of anthropogenic climate change are likely to some degree sensitive to the anthropogenic background trend.

Consideration of broader forcing uncertainties.
In the earlier discussion limitations arising from ensemble size were discussed in the context of the specific challenge of volcanic forcing. If in addition it is desired to consider various plausible future anthropogenic forcing scenarios the challenge becomes yet more acute. Future work should aim at optimizing the experimental design to answer as many scientific and societally relevant questions as possible while ensuring statistical robustness and simultaneously minimizing computational costs.

Specifically, our experimental design does not consider uncertainties in other external forcings. Differences in our results for the late 21st century versus the entire period demonstrate that the relative importance of volcanic impact depends on the anthropogenic forcing trajectory (Fig. 3d-e). In addition to using a single anthropogenic forcing scenario in our experiments, historical solar variability was repeated as suggested in the latest climate projection protocols[32]. A similar approach as the one presented for volcanic uncertainty could be used to assess solar forcing uncertainty effects in future climate projections. This would be more involved as it would need to properly account for the long-term memory processes readily apparent in available solar reconstructions and the broad uncertainty apparent in the range of available historical estimates.

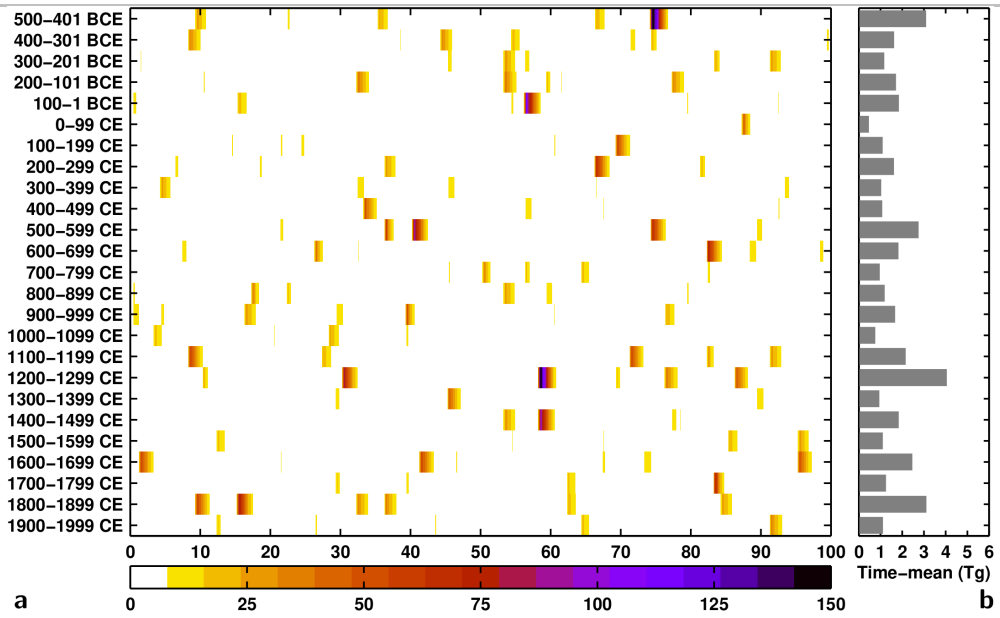

Supplementary Fig. 1 | **Historical volcanic forcing. a**, Stratospheric volcanic aerosol load (Tg) reconstructed from sulphate depositions over the last 2,500 years in Greenland and Antarctic ice-cores[4]. Centuries on y-axis and year of century on x-axis. **b**, Centennial mean load.

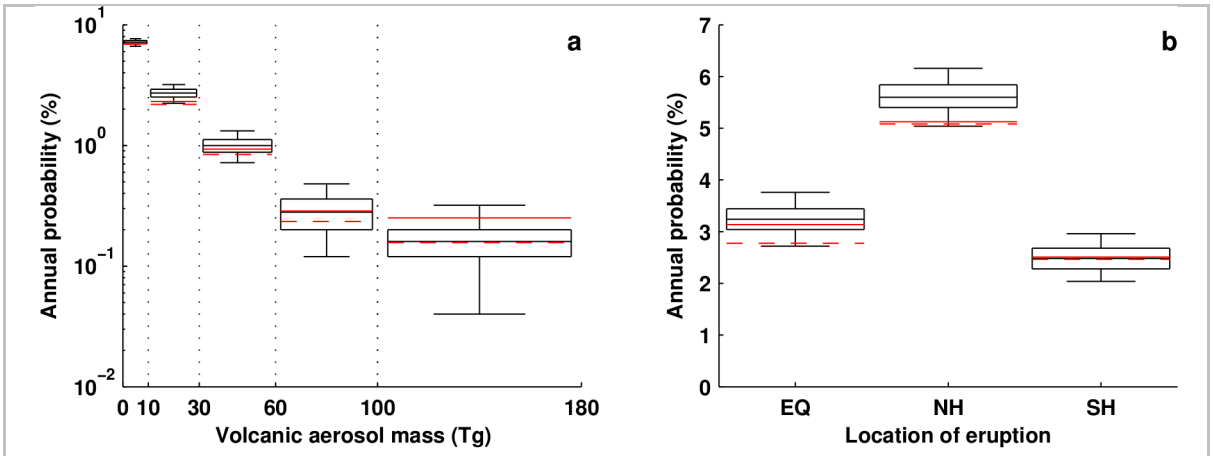

Supplementary Fig. 2 | **Eruption size and location statistics. a**, Annual eruption probabilities for selected size classes derived from Sigl et al.[4] reconstruction (black), VOLC forcing futures (solid red) and VOLC forcing futures after removing the five strongest forcing members (stippled red). Sample uncertainties for the reconstructed data are indicated by 5-95 and 25-75 bootstrap-percentiles (box-whiskers). **b**, As **a**, but for location of eruptions.

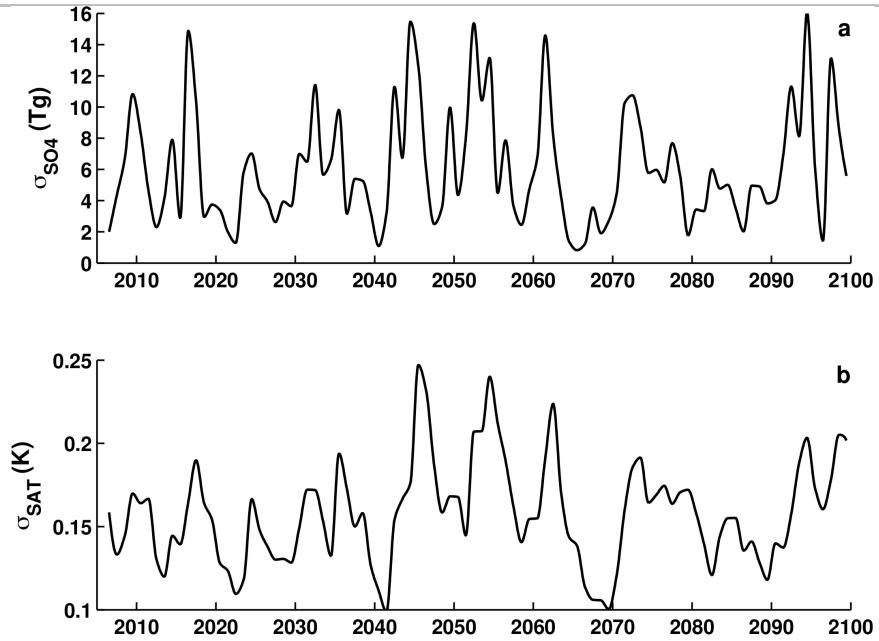

Supplementary Fig. 3 | **Ensemble spread of global temperature versus ensemble spread of volcanic aerosol load. a,** Ensemble standard-deviation of annual mean stratospheric volcanic aerosol load. **b,** Ensemble standard-deviation of global mean surface air temperature. Correlation coefficient r=0.6 for lag 0 and r=0.75 for lag 1 (aerosol forcing leading).

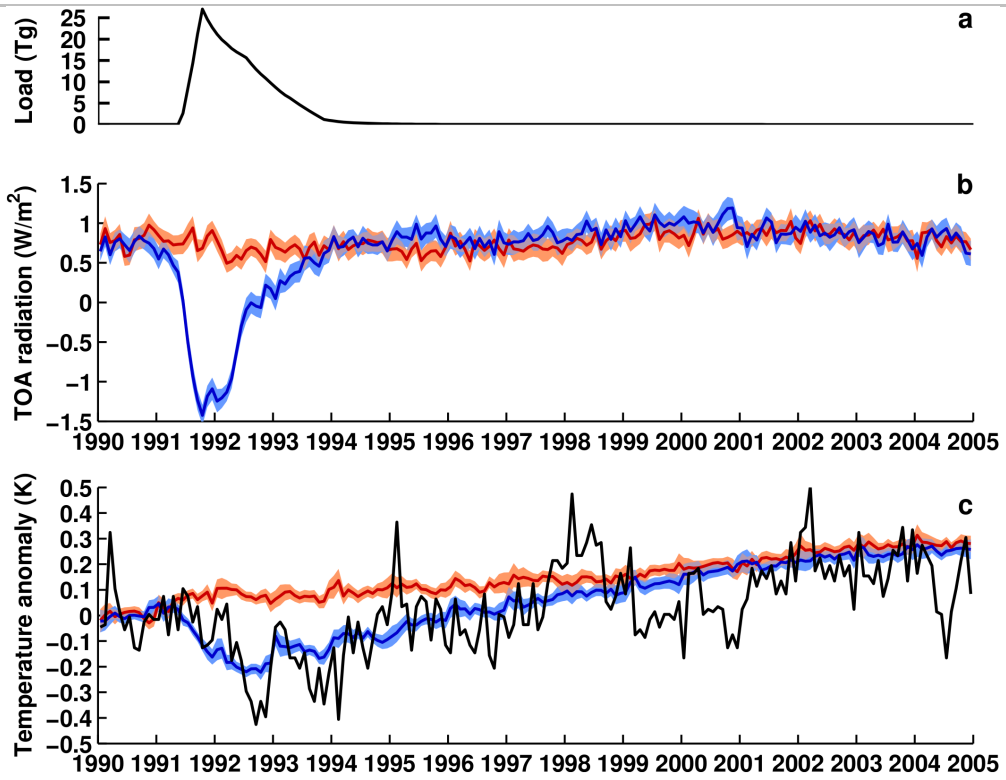

Supplementary Fig. 4 | **Radiation and temperature response to Mt. Pinatubo eruption. a,** Stratospheric volcanic aerosol load in NorESM's historical simulation, **b,** Top-of-atmosphere net radiation balance (negative up) from 60 simulations with (blue) and without (red) Mt. Pinatubo forcing. Monthly values with seasonal cycle removed of ensemble means (solid), with 5-95% bootstrap confidence bounds (shading). **c,** Global surface temperature change relative to 1990. The NASA GISS observational global temperature estimate[33] (black) is shown for comparison.

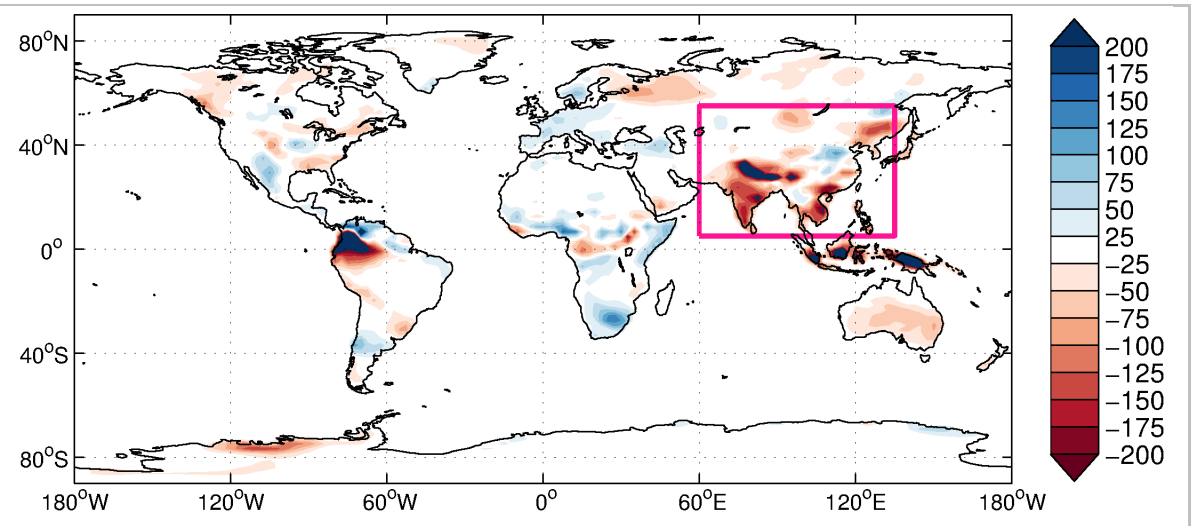

Supplementary Fig. 5 | **Boreal summer precipitation response to Mt. Pinatubo eruption.** Ensemble mean difference for 1992 May–September averaged precipitation over land, computed from the output of 60 historical NorESM simulations with and without Mt. Pinatubo forcing. Units are in mm/yr. The box (5–55ºN, 60–135ºE) marks the region Feng et al.[17] used for defining their warm season Asian precipitation index.

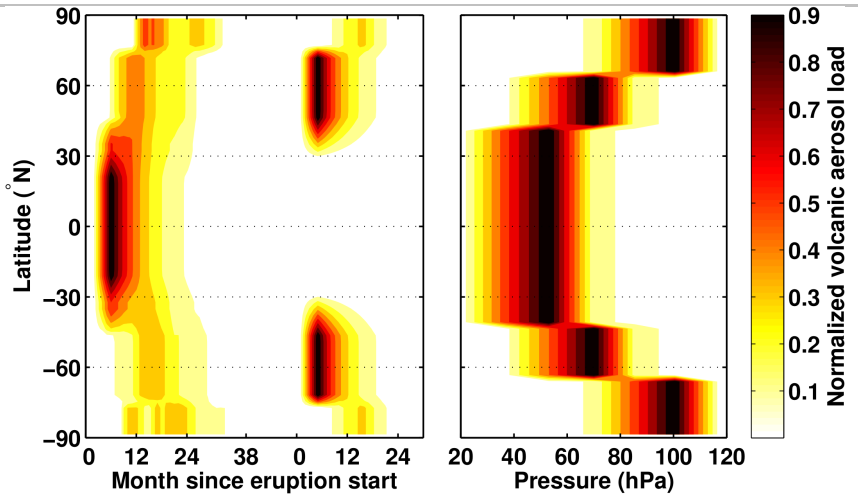

Supplementary Fig. 6 | **Spatiotemporal shape functions of volcanic forcing.** Normalized latitude-time (left) and latitude-height (right) shape functions.

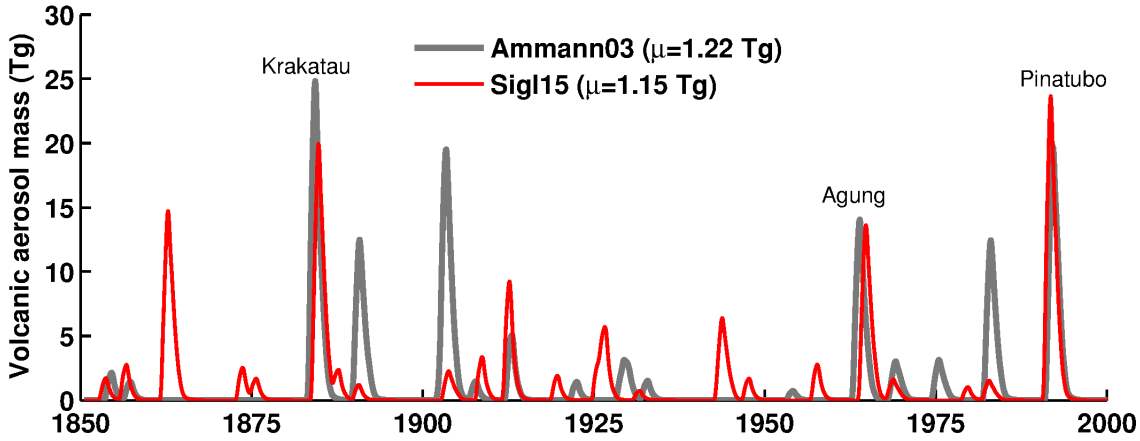

Supplementary Fig. 7 | **CMIP5 versus ice-core reconstructed volcanic forcing of the recent past.** Forcing from the model's CMIP5 historical integration[34] (gray) versus an ice-core based reconstruction[4] (red) as described in Methods.

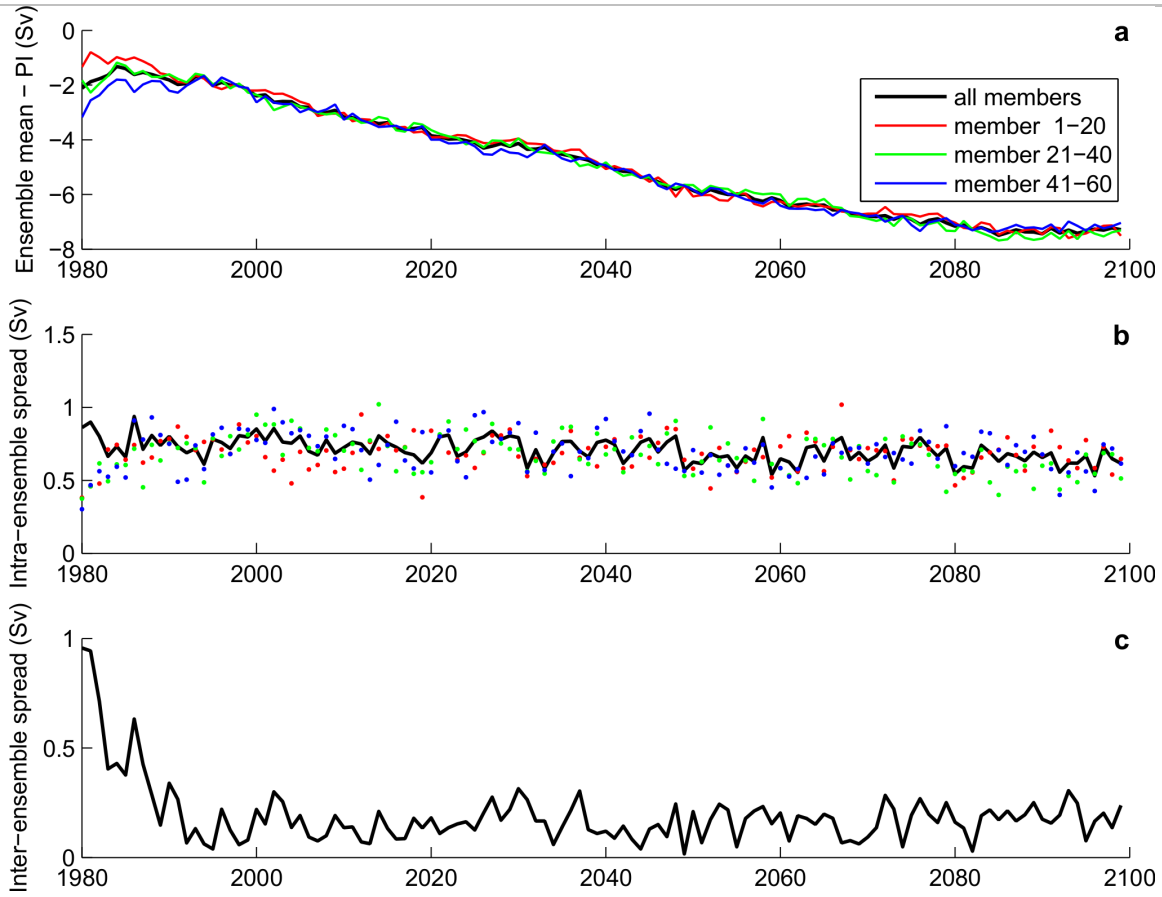

Supplementary Fig. 8 | **Evolution of AMOC spread in SPINUP and NO-VOLC. a,** Mean over subsets of members relative to pre-industrial (PI). **b,** Intra-subset standard-deviation. **c,** Inter-subset standard-deviation computed from the three subset means. The Atlantic Meridional Overturning Circulation (AMOC) strength is evaluated at 26ºN.

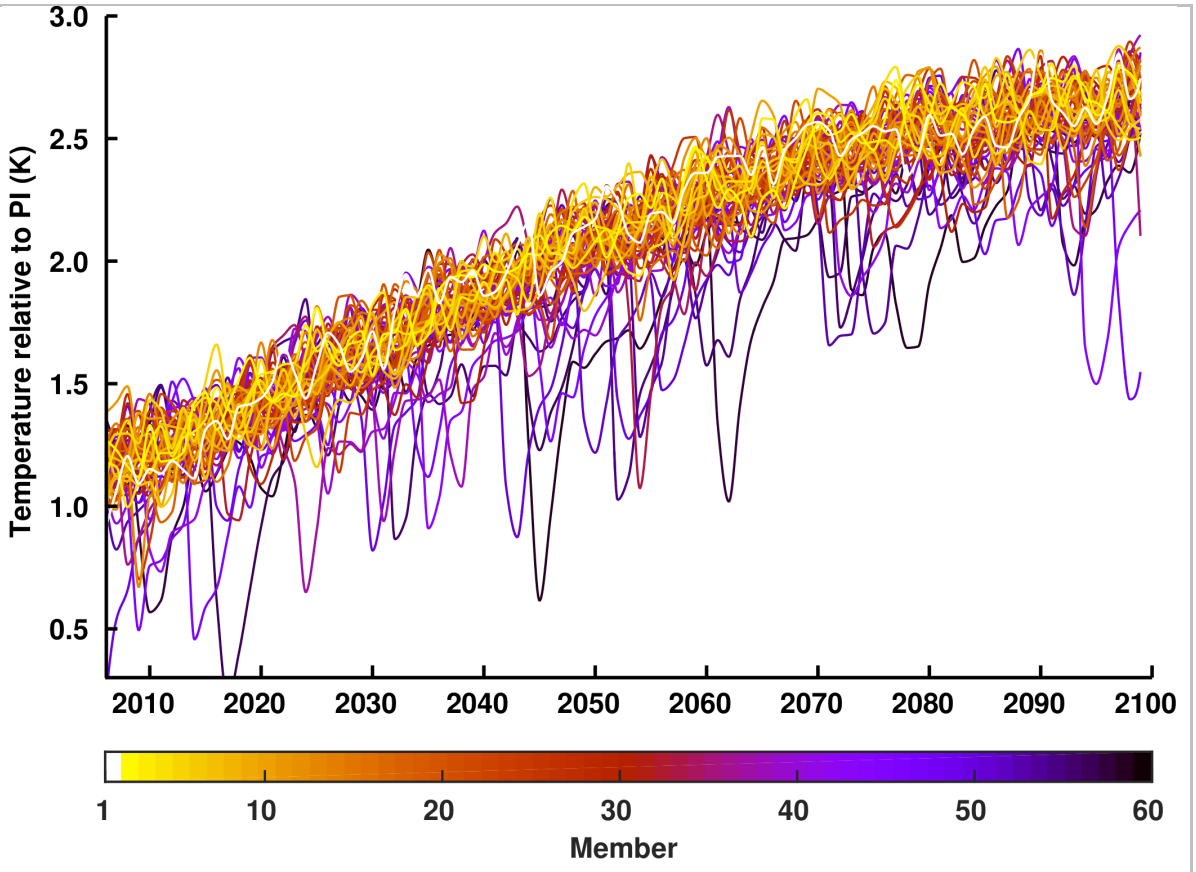

Supplementary Fig. 9 | **Annual-mean GMST of individual VOLC ensemble members.** Members are ranked according to their centennial-mean volcanic forcing. Temperatures are relative to the model's pre-industrial (PI) reference climate.

Supplementary Table 1 | **Changes in distribution statistics.** The distribution statistics presented in the table complement the analyses of the main article and are computed along the ensemble dimension and where applicable, also time dimension. Means are computed relative to the year-1850 model climate. Standard-deviations are computed after subtracting the time dependent ensemble-mean. Number in brackets denote 5-95% bootstrap confidence intervals.

Variable	Stats	Units	NO-VOLC	VOLC-CONST	VOLC
Fig. 2 – Annual SAT					
All years	mean	K	2.08 (2.07 - 2.09)	2.02 (2.00 - 2.04)	2.01 (2.00 - 2.02)
	std	K	0.092 (0.090 - 0.093)	0.089 (0.086 - 0.092)	0.159 (0.146 - 0.172)
2016–2035 mean	mean	K	1.58 (1.57 - 1.59)	1.52 (1.53 - 1.54)	1.52 (1.51 - 1.54)
	std	K	0.032 (0.028 - 0.035)	0.032 (0.024 - 0.039)	0.075 (0.056 - 0.091)
dSAT > 1.5K	mean	yr	2022.3 (2022.0 - 2022.5)	2024.3 (2023.8 - 2024.8)	2024.3 (2023.7 - 2025.0)
	std	yr	1.3 (1.1 - 1.5)	1.5 (1.0 - 1.8)	3.0 (2.4 - 3.6)
Fig. 3 – Decadal SAT					
10-yr means	std	K	0.039 (0.037 - 0.041)	0.041 (0.038 - 0.044)	0.109 (0.097 - 1.121)
10-yr trends	mean	K/10-yr	0.17 (0.17 - 0.18)	0.16 (0.16 - 0.17)	0.17 (0.16 - 0.17)
	std	K/10-yr	0.123 (0.118 - 0.127)	0.128 (0.121 - 0.136)	0.238 (0.216 - 0.261)
	P(y<0)	%	10.4 (9.6 - 11.2)	11.4 (9.8 - 13.0)	16.8 (15.7 - 17.9)
	P(y<0) [a]	%	4.2 (3.2 - 5.3)	4.6 (3.0 - 6.1)	10.5 (8.5 - 12.5)
Fig. 4 – Decadal averages					
TOA net	mean	W/m2	1.26 (1.26 - 1.27)	1.23 (1.22 - 1.23)	1.21 (1.20 - 1.22)
	std	W/m2	0.06 (0.06 - 0.07)	0.06 (0.06 - 0.07)	0.21 (0.18 - 0.24)
Sea level	mean	mm	139.3 (138.7 - 139.9)	135.3 (134.4 - 136.3)	134.1 (132.9 - 135.2)
	std	mm	3.2 (2.9 - 3.4)	3.4 (3.0 - 3.7)	7.0 (6.0 - 7.8)
Monsoon precip.	mean	mm/yr	48.0 (46.9 - 49.2)	41.7 (40.2 - 43.1)	40.8 (39.2 - 42.4)
	std	mm/yr	15.6 (14.9 - 16.4)	16.3 (14.9 - 17.7)	19.1 (18.1 - 19.9)
AMOC strength	mean	Sv	-4.34 (-4.36 - -4.31)	-4.20 (-4.25 - -4.15)	-4.12 (-4.16 - -4.08)
	std	Sv	0.41 (0.39 - 0.43)	0.46 (0.40 - 0.50)	0.50 (0.47 - 0.53)
NH sea ice volume	mean	10^{12} m3	-28.4 (-28.5 - -28.3)	-28.1 (-28.3 - -27.9)	-27.9 (-28.1 - -27.7)
	std	10^{12} m3	1.3 (1.2 - 1.4)	1.4 (1.2 - 1.6)	1.5 (1.4 - 1.7)

[a] analysis limited to 2005–2050

Supplementary Table 1 | **Continued.** The computation of VOLC55 statistics omits the simulation results from the five strongest forcing members shown in Figure 1.

Variable	Stats	Units	VOLC	VOLC55
Fig. 2 – Annual SAT				
All years	mean	K	2.01 (2.00 - 2.02)	2.02 (2.01 - 2.03)
	std	K	0.159 (0.146 - 0.172)	0.147 (0.136 - 0.158)
2016–2035 mean	mean	K	1.52 (1.51 - 1.54)	1.53 (1.51 - 1.55)
	std	K	0.075 (0.056 - 0.091)	0.068 (0.050 - 0.083)
dSAT > 1.5K	mean	yr	2024.3 (2023.7 - 2025.0)	2024.1 (2023.5 - 2024.8)
	std	yr	3.0 (2.4 - 3.6)	3.0 (2.2 - 3.6)
Fig. 3 – Decadal SAT				
10-yr means	std	K	0.109 (0.097 - 1.121)	0.095 (0.085 - 0.104)
10-yr trends	mean	K/10-yr	0.17 (0.16 - 0.17)	0.17 (0.16 - 0.17)
	std	K/10-yr	0.238 (0.216 - 0.261)	0.214 (0.196 - 0.232)
	P(y<0)	%	16.8 (15.7 - 17.9)	16.0 (15.0 - 17.0)
	P(y<0) [a]	%	10.5 (8.5 - 12.5)	9.4 (7.5 - 11.3)
Fig. 4 – Decadal averages				
TOA net	mean	W/m2	1.21 (1.20 - 1.22)	1.22 (1.21 - 1.22)
	std	W/m2	0.21 (0.18 - 0.24)	0.19 (0.16 - 0.21)
Sea level	mean	mm	134.1 (132.9 - 135.2)	134.9 (133.7 - 136.0)
	std	mm	7.0 (6.0 - 7.8)	6.2 (5.2 - 7.2)
Monsoon precip.	mean	mm/yr	40.8 (39.2 - 42.4)	42.0 (40.6 - 43.4)
	std	mm/yr	19.1 (18.1 - 19.9)	18.3 (17.5 - 19.1)
AMOC strength	mean	Sv	-4.12 (-4.16 - -4.08)	-4.14 (-4.18 - -4.10)
	std	Sv	0.50 (0.47 - 0.53)	0.49 (0.46 - 0.52)
NH sea ice volume	mean	10^{12} m3	-27.9 (-28.1 - -27.7)	-27.9 (-28.1 - -27.8)
	std	10^{12} m3	1.5 (1.4 - 1.7)	1.5 (1.4 - 1.7)

[a] analysis limited to 2005–2050

Supplementary References

1. Gao, C., Oman, L., Robock, A. & Stenchikov, G. L. Atmospheric volcanic loading derived from bipolar ice cores: Accounting for the spatial distribution of volcanic deposition. *J. Geophys. Res.* **112,** D09109 (2007).
2. Crowley, T. J. & Unterman, M. B. Technical details concerning development of a 1200 yr proxy index for global volcanism. *Earth Syst. Sci. Data* **5**, 187–197 (2013).
3. Sigl, M. *et al*. A new bipolar ice core record of volcanism from WAIS Divide and NEEM and implications for climate forcing of the last 2000 years. *J. Geophys. Res. Atmos.* **118**, 1151–1169 (2013).
4. Sigl, M. *et al*. Timing and climate forcing of volcanic eruptions for the past 2,500 years. *Nature* **523,** 543–549 (2015).
5. Timmreck, C. *et al*. Aerosol size confines climate response to volcanic super-eruptions. *Geophys. Res. Lett.* **37** (2010).
6. Wilson, R. *et al*. Last millennium northern hemisphere summer temperatures from tree rings: Part I: The long term context, *Quat. Sci. Rev.* **134** (2016).
7. Naveau, P. & Ammann, C. M. Statistical distributions of ice core sulfate from climatically relevant volcanic eruptions. *Geophys. Res. Lett.* **32**, L05711 (2005)
8. Ammann, C. M. & Naveau, P. A statistical volcanic forcing scenario generator for climate simulations. *J. Geophys. Res.* **115,** D05107 (2010).
9. Self, S. & Gertisser, R. Tying down eruption risk. *Nat. Geosci.* **8,** 248–250 (2015).
10. Zanchettin, D. *et al*. Background conditions influence the decadal climate response to strong volcanic eruptions. *J. Geophys. Res. Atmos.* **118,** 4090–4106 (2013).
11. Pausata, F. S. R., Grini, A., Caballero, R., Hannachi, A. & Seland, Ø. High-latitude volcanic eruptions in the Norwegian Earth System Model: the effect of different initial conditions and of the ensemble size. *Tellus B* **67,** (2015).
12. Minnis, P. et al. Radiative Climate Forcing by the Mount Pinatubo Eruption. *Science* **259**, 1411–1415 (1993).
13. Driscoll, S., Bozzo, A., Gray, L. J., Robock, A. & Stenchikov, G. Coupled Model Intercomparison Project 5 (CMIP5) simulations of climate following volcanic eruptions. *J. Geophys. Res. Atmos.* **117,** D17105 (2012).
14. Santer, B. D. et al. Accounting for the effects of volcanoes and ENSO in comparisons of modeled and observed temperature trends. *J. Geophys. Res. Atmos.* **106**, 28033–28059 (2001).
15. Thompson, D. W. J. et al. Identifying Signatures of Natural Climate Variability in Time Series of Global-Mean Surface Temperature: Methodology and Insights. *J. Clim.* **22**, 6120–6141 (2009).
16. Soden, B.J., Wetherald, R.T., Stenchikov, G.L. & Robock L. Global Cooling After the Eruption of Mount Pinatubo: A Test of Climate Feedback by Water Vapor. Science 292, 727–730 (2002).
17. Feng, S. *et al*. A Gridded Reconstruction of Warm Season Precipitation for Asia Spanning the Past Half Millennium. *J. Clim.* **26,** 2192–2204 (2013).
18. Liu, F. *et al*. Global monsoon precipitation responses to large volcanic eruptions. *Sci. Rep.* **6,** 24331 (2016).
19. Haywood, J. M., Jones, A., Bellouin, N. & Stephenson, D. Asymmetric forcing from stratospheric aerosols impacts Sahelian rainfall. *Nat. Clim. Chang.* **3,** 660–665 (2013).
20. Iles, C. E. *et al*. The global precipitation response to volcanic eruptions in the CMIP5 models. *Environ. Res. Lett.* **9,** 104012 (2014).

21. Stenchikov, G. *et al*. Arctic Oscillation response to volcanic eruptions in the IPCC AR4 climate models. *J. Geophys. Res.* **111,** D07107 (2006).
22. Zambri, B. & Robock, A. Winter warming and summer monsoon reduction after volcanic eruptions in Coupled Model Intercomparison Project 5 (CMIP5) simulations. *Geophys. Res. Lett.* **43,** 10,920-10,928 (2016).
23. Bittner, M., Schmidt, H., Timmreck, C. & Sienz, F. Using a large ensemble of simulations to assess the Northern Hemisphere stratospheric dynamical response to tropical volcanic eruptions and its uncertainty. *Geophys. Res. Lett.* **43,** 9324–9332 (2016).
24. Charlton-Perez, A. J. *et al*. On the lack of stratospheric dynamical variability in low-top versions of the CMIP5 models. *J. Geophys. Res. Atmos.* **118,** 2494–2505 (2013).
25. Iversen, T. *et al*. The Norwegian Earth System Model, NorESM1-M – Part 2: Climate response and scenario projections. *Geosci. Model Dev.* **6,** 389–415 (2013).
26. Swingedouw, D. *et al*. Bidecadal North Atlantic ocean circulation variability controlled by timing of volcanic eruptions. *Nat. Commun.* **6,** 6545 (2015).
27. Self, S., Rampino, M. R., Zhao, J. & Katz, M. G. Volcanic aerosol perturbations and strong El Niño events: No general correlation. *Geophys. Res. Lett.* **24,** 1247–1250 (1997).
28. Pausata, F. S. R., Chafik, L., Caballero, R. & Battisti, D. S. Impacts of high-latitude volcanic eruptions on ENSO and AMOC. *Proc. Natl. Acad. Sci.* **112,** 201509153 (2015).
29. Vuuren, D. P. *et al*. The representative concentration pathways: an overview. *Clim. Change* **109,** 5–31 (2011).
30. Mitchell, D. *et al*. Half a degree additional warming, prognosis and projected impacts (HAPPI): Background and experimental design. *Geosci. Model Dev.* **10,** (2017).
31. Knutti, R. & Sedlacek, J. Robustness and uncertainties in the new CMIP5 climate model projections. *Nat. Clim. Chang.* **3,** 369–373 (2013).
32. O'Neill, B. C. *et al*. The Scenario Model Intercomparison Project (ScenarioMIP) for CMIP6. *Geosci. Model Dev.* **9,** 3461–3482 (2016).
33. Hansen, J., Ruedy, R., Sato, M. & Lo, K. Global surface temperature change. *Rev. Geophys.* **48,** RG4004 (2010).
34. Ammann, C. M., Meehl, G. A., Washington, W. M. & Zender, C. S. A monthly and latitudinally varying volcanic forcing dataset in simulations of 20th century climate. *Geophys. Res. Lett.* **30,** 1657 (2003).

Matlab code for generating proxy-based volcanic forcing futures

```
% created 12 Oct 2016 (ingo.bethke@uni.no)

% read sulphate depositions from SI of Sigl et al. 2015, Nature
data=xlsread('nature14565-s6.xlsx',2);

% set missing data to zero
data(isnan(data))=0;

% extract fields
location_sigl15=data(:,2); % location flag (1=tropical, 2=NH, 3=SH)
deposition_north=data(:,3); % Greenland
deposition_south=data(:,5); % Antarctica

% convert to stratospheric volcanic aerosol mass (Tg) using
% scaling relation from Gao et al. 2007, J. Geophys. Res.
for n=1:length(location_sigl15)
  if location_sigl15(n)==2
    mass_sigl15(n)=0.57*deposition_north(n);
  else
    mass_sigl15(n)=deposition_north(n)+deposition_south(n);
  end
end

% define ensemble size and time period for synthetic forcing
NMEMBER=60; % number of forcing members
YEAR1=2006;
YEARN=2099;
P=1./2500./12.; % probability for eruption to occur in specific month

% choose and seed random number generator
%   The twister algorithm is default in python and new matlab versions.
%   The below setting gives the same result as the numpy python
%   implementation.
rand('twister',0);

% create forcing futures
for member=1:NMEMBER
  count_future=0;
  for y=YEAR1:YEARN
    for m=1:12
      for count_sigl15=1:length(mass_sigl15)
        if rand<P
          count_future=count_future+1;
          year{member}(count_future)=y;
          month{member}(count_future)=m;
          location{member}(count_future)=location_sigl15(count_sigl15);
          mass{member}(count_future)=mass_sigl15(count_sigl15);
        end
      end
    end
  end
end

% save result
save futureVolcForcing.mat year month location mass
```